الجمهورية الجزائرية الديمقراطية الشعبية

People's Democratic Republic of Algeria

وزارة التعليم العالي والبحث العلمي

Ministry of Higher Education and Scientific Research

جامعة غرداية

University of Ghardaia

كلية العلوم والتكنولوجيا

Faculty of Science and Technology

قسم الآلية والكهروميكانيك

Department of Automatics and Electromechanics

Final Thesis Submitted in partial fulfillment of the requirements for the degree of

Bachelor

Field of Study: Science and Technology
Specialization: Renewable Energy and the Environment

Title

Solid-state hydrogen storage: Theoretical study of $ScPd_3H_4$ hydride

Presented by:

BEN GHENIA Bouchra and RECIOUI Imane

Defended publicly on: 13 /06/2026

Board of Examiners:

REBAI Aissa	Professor	Univ. Ghardaia	**President**
HASSAN Nacer	Professor	Univ. Ghardaia	**Examiner**
BOUHADDA Youcef	Research Director	URAER /CDER Ghardaia	**Supervisor**
AZZAOUI Mohammed	Professor	Univ. Ghardaia	**Co-supervisor**

Academic Year: 2026 / 2025

Acknowledgment

First and foremost, all praise and thanks are due to Allah, the Almighty, for granting us the strength, patience, and guidance to successfully complete this work.

We would like to express our deepest gratitude to our beloved parents for their unconditional love, endless support, sacrifices, and constant encouragement throughout our academic journey. To them, we dedicate the fruit of this work with all our love and appreciation.

We also extend our sincere thanks to each other, as partners in this journey, for our cooperation, shared efforts, perseverance, and mutual support, which made the completion of this dissertation possible.

Our heartfelt appreciation goes to our supervisor for his invaluable guidance, continuous encouragement, patience, and constructive advice throughout every stage of this research. His support and expertise have been essential to the successful completion of this work.

We would also like to express our sincere gratitude to the Chair of the Examination Committee and the distinguished members of the examination committee for accepting to evaluate this dissertation and for their valuable comments, constructive suggestions, and insightful remarks, which have greatly contributed to improving the quality of this work.

Our sincere appreciation is also extended to all the administrative staff of the ***Faculty of Science and Technology****, especially those of the* ***Department of Mechanical Engineering and Electromechanics****, for their cooperation, kindness, and assistance in facilitating the administrative procedures and providing the necessary official documents throughout our academic journey.*

Finally, we would like to thank our family, friends, and everyone who supported, encouraged, or assisted us in any way during the preparation of this dissertation. Their encouragement and confidence in us have been a constant source of motivation.

We sincerely hope that this work will contribute, even modestly, to scientific knowledge and benefit future researchers in this field.

Abstract

In the present study, we present a comprehensive theoretical study of the structural, mechanical, optical, and thermodynamic properties of $ScPd_3$ and its hydride $ScPd_3H_4$ for potential applications in solid-state hydrogen storage. This analysis is presented using the CASTEP software, based on density functional theory (DFT).

Our calculations show that geometric optimization confirmed the experimental lattice parameters of these materials and the stability of the studied structures after hydrogen incorporation.

The calculated electronic structure revealed that $ScPd_3$ and $ScPd_3H_4$ exhibit metallic character, indicating that hydrogen insertion does not affect the nature of the chemical bond. However, this study shows that hydrogen influences certain optical properties (polarizability and absorption).

The enthalpy of formation (ΔH_f) of the $ScPd_3H_4$ compound has been calculated and is found to be 37.31 kJ/mol·H_2 lower than that of some hydrogen storage materials. This is favorable for stationary hydrogen storage applications.

Keywords: Hydrogen-solid-state storage, $ScPd_3$, $ScPd_3H_4$, DFT, electronic structure, hydrides.

Résumé

Dans la présente étude, nous présentons une étude théorique complète des propriétés structurelles, mécaniques, optiques et thermodynamiques de $ScPd_3$ et de son hydrure $ScPd_3H_4$ pour des applications potentielles dans le stockage de l'hydrogène à l'état solide. Cette analyse est effectuée à l'aide du logiciel CASTEP, basé sur la théorie de la fonctionnelle de la densité (DFT). Nos calculs montrent que l'optimisation géométrique a confirmé les paramètres de maille expérimentaux et la stabilité des structures après l'incorporation d'hydrogène. La structure électronique révèle un caractère métallique pour $ScPd_3$ et $ScPd_3H_4$, indiquant que l'insertion d'hydrogène n'affecte pas la nature de la liaison chimique, bien qu'elle influence certaines propriétés optiques. L'enthalpie de formation (ΔHf) de $ScPd_3H_4$ est de 37,31 kJ/mol·H_2, ce qui est favorable pour le stockage stationnaire.

Mots-clés : Stockage de l'hydrogène, $ScPd_3$, $ScPd_3H_4$, DFT, structure électronique, hydrures.

الملخص

في هذه الدراسة، نقدم دراسة نظرية شاملة للخواص البنيوية والميكانيكية والبصرية والديناميكية الحرارية لمركب $ScPd_3$ وهيدريده$ScPd_3H_4$ ، وذلك لتطبيقاتهما المحتملة في تخزين الهيدروجين في الحالة الصلبة. وقد تم إجراء هذا التحليل باستخدام برنامجCASTEP ، استنادًا إلى نظرية الكثافة الوظيفية (DFT) .

تُظهر حساباتنا أن التحسين الهندسي قد أكد معلمات الشبكة التجريبية لهذه المواد، بالإضافة إلى استقرار البنى المدروسة بعد إدخال الهيدروجين.

كشفت البنية الإلكترونية المحسوبة أن $ScPd_3$ و $ScPd_3H_4$يتميزان بخواص معدنية، مما يشير إلى أن إدخال الهيدروجين لا يؤثر على طبيعة الرابطة الكيميائية. ومع ذلك، تُظهر هذه الدراسة أن الهيدروجين يؤثر على بعض الخواص البصرية (الاستقطابية والامتصاص).

تم حساب إنثالبي التكوين (ΔH_f) لمركب$ScPd_3H_4$ ، ووجد أنه أقل بمقدار 37.31 كيلوجول/مول H_2•من إنثالبي التكوين لبعض مواد تخزين الهيدروجين. وهذا يُعدّ ميزةً لتطبيقات تخزين الهيدروجين الثابتة.

تم حساب إنثالبي التكوين (ΔH_f) لمركب$ScPd_3H_4$ ، ووجد أنه أقل بمقدار 37.31 كيلوجول/مول H_2•من إنثالبي التكوين لبعض مواد تخزين الهيدروجين. وهذا يُعدّ ميزةً لتطبيقات تخزين الهيدروجين الثابتة.

الكلمات المفتاحية: تخزين الهيدروجين في الحالة الصلبة، $ScPd_3$، $ScPd_3H_4$، نظرية الكثافة الوظيفية، البنية الإلكترونية، الهيدريدات.

Contents

List of Figures

List of Tables

Introduction

Hydrogen is emerging as a key component of the transition toward renewable energy systems since it has the capability of being used progressively in place of fossil fuel. The interest in using hydrogen as an alternative to fossil fuels is demonstrated by the fact that the total demand for hydrogen around the world was 97 million tonnes in 2023. However, it is expected to be greater than 100 million tonnes by 2025, reflecting an increasing awareness among various segments of industry regarding this form of energy.

It is also well known that dependence upon fossil fuels makes global economies extremely susceptible to major geo-political conflicts. For example: the Russia-Ukraine and U.S.-Venezuela crises, along with the most recent attack on Iran, have produced major upheavals in energy markets, which have resulted in changes to the way petroleum (and natural gas) are distributed, increased costs associated with transporting energy products and higher overall energy costs.

Therefore, there exists an urgent need to develop new forms of energy and reduce dependency upon fossil fuels. Furthermore, the overwhelming use of fossil fuels creates both serious air pollution and contributes to global warming through the emission of greenhouse gases. On the other hand, burning hydrogen produces only water vapor and energy compared to coal or oil. thus providing a means for reducing the amount of greenhouse gas emitted into the atmosphere and achieving the goal of limiting warming to 1.5 degrees C. in addition to that, hydrogen has a high storage energy capacity compared to fossil fuels such as: gasoline, diesel, GNL…etc.

However, the main challenge of the widespread use of hydrogen is the method of storing and transporting it safely and efficiency. This has prompted researchers in this field to develop and discover other methods capable of overcoming this challenge. Among these promising methods for storing hydrogen, solid materials can be considered the best candidate due to its capacity of storing hydrogen by absorbing or trapping it within their crystalline structure. In this context, intermetallic compounds have emerged as a promising option, as they possess a regular crystalline structure and tenable physical properties. These compounds appear in different classes that have the ability to be mechanically and to store high amount of hydrogen.

The AB_3 family can be a good model for study as it combines a rare-earth element (A), giving it unique properties, with a transition element (B) that contributes to improving its electronic properties. Among them, $ScPd_3$ take attention due in its excellent reactivity with hydrogen, forming a hydride ($ScPd_3H_4$). This hydride has a stable cubic structure, allowing hydrogen atoms to enter the interfacial positions without disrupting the compound's fundamental structure. However, this absorption leads to significant changes such as crystal size and strong change in the bonding between atoms. However, the effect of hydrogen insertion in $ScPd_3$, on electronic, optical and thermodynamic properties have not been studied before even experimentally or theoretically.

Therefore, in the present work, we studied the structural, mechanical, electronic, optical and thermodynamic properties of both $ScPd_3$ and $ScPd_3H_4$ materials. We have used the CASTAP software, based on Density Functional Theory (DFT). In fact, DFT is considered one of the best tools to investigate electronic, optical, and mechanical properties in material science. This theory, which based on the principles of quantum mechanics and only on atomic structure, can describe the behavior of electrons in materials and can predict the above properties without complex laboratory experiments.

This manuscript is structured as follows:

- Chapter 1 presents the hydrogen sector, beginning with the question "Why hydrogen?" followed by an examination of hydrogen's properties, production, transport, and storage. It also includes a brief description of the various characteristics and aspects of the metal-hydrogen system and the main hydrogen-absorbing metal systems and families. Finally, there is a short introduction to the concepts and theoretical foundations of the calculation method used, namely DFT theory.
- Chapter 2 presents the results obtained using ab initio methods for the study of the $ScPd_3$-hydrogen system.

Finally, a conclusion summarizes the main results of our work.

1 Chapter 1

1.1 Introduction

In this chapter, we present the strong arguments for shifting towards hydrogen usage. Certainly, the advancement of clean hydrogen serves not only as a solution to environmental issues but also as a geopolitical approach to enhance global energy security.

1.2 Why hydrogen

1.2.1 Geopolitical problems of energy

Fossil fuels are among the most important elements on which global energy systems depend, such as oil and natural gas, which in turn are concentrated in limited geographical areas such as (Iraq, Venezuela, Saudi Arabia and Canada), and this concentration creates risks geopolitical factors, and consequently instability in supplies and price fluctuations, threaten global energy security (figure 1-1). The dependence of major countries with strong global power leads to potential competition among them, which puts energy prices and international market fluctuations under the weight of these conflicts and tensions.

Here, hydrogen stands out as one strategic alternative, as it can be produced locally using renewable sources [1].

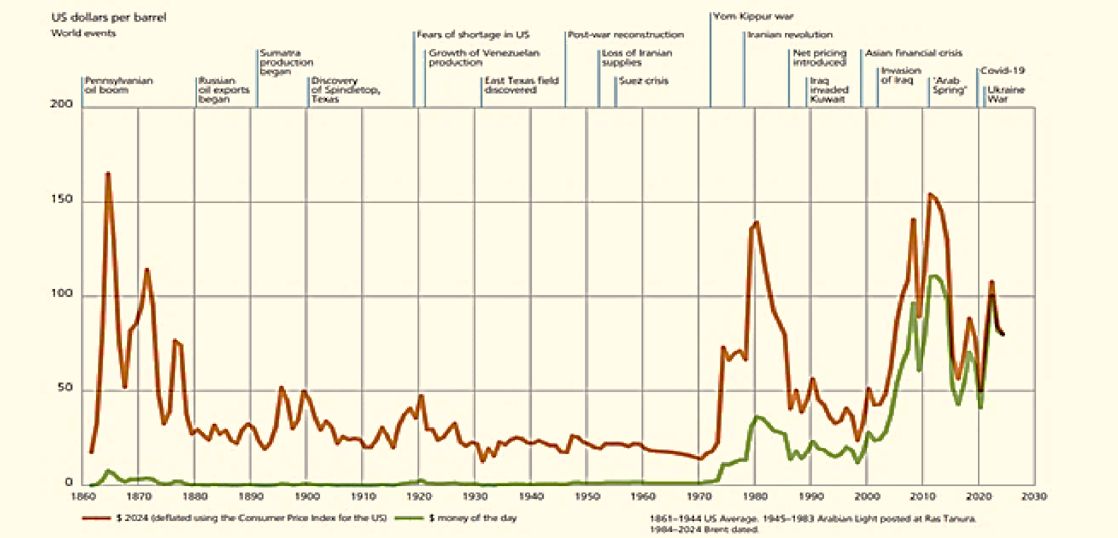

Figure 1-1: Fluctuations in oil prices during the period 1860-2030 [2].

1.2.2 Environmental problems

What the 21st century is witnessing today in terms of climate change due to human activities, especially the burning of fossil fuels and deforestation, is the main reason for the recorded rise in the average temperature of the Earth (figure 1-2). Indeed, since 1970, global warming has proceeded at a roughly linearly.

Therefore, the effect of global warming stands out as one of the direct results of the increasing emissions of warming gases such as water vapor, Carbon dioxide, methane (CH_4), and nitrous oxide (N_2O) [3-4]. Today's energy systems are heavily focused on reducing carbon intensity through a transition to low-emission or zero-emission energy sources such as renewable energy sources. This will require tremendous efforts to transform the energy sector in the coming decades [1].

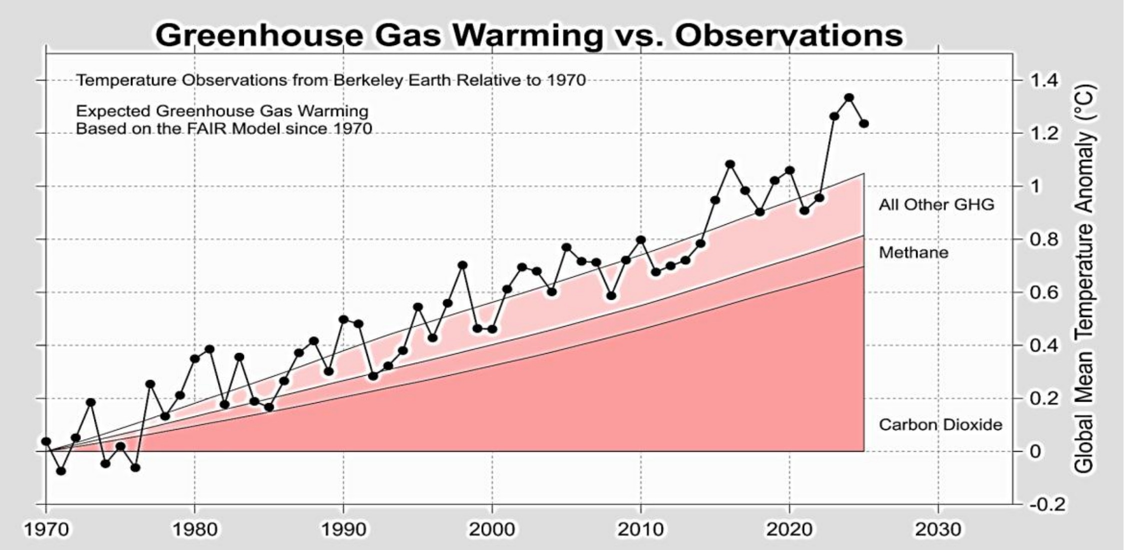

Figure 1-2 :Greenhouse gas warming and global temperature anomaly [5]

1.3 Hydrogen

Hydrogen was discovered in 1766 by the British scientist Henry Cavendish, who presented a study before the Royal Society of London entitled On Factitious Airs. He demonstrated the existence of gases different from ordinary air and succeeded in isolating what he called “inflammable air,” which was later identified as hydrogen gas. He also observed that it was about ten times lighter than atmospheric air [6]. In 1783, the French chemist Antoine Lavoisier confirmed Cavendish’s findings and proposed the name “Hydrogen” instead of “inflammable air.” The term is derived from Greek: Hydro (water) and General (to produce), meaning “water former,” after it was demonstrated that the combination of hydrogen and oxygen produces water. Hydrogen is the most abundant element in the universe, representing about 75% of the total mass and nearly 92% of the number of atoms. It exists in vast quantities in stars, gaseous planets, nebulae, and interstellar gases. On Earth, it is not found in significant free quantities but mainly occurs in compounds such as water (H_2O) and organic materials. Therefore, hydrogen is not a primary energy source; it must be produced before it can be used [6].

Hydrogen has a high gravimetric energy density, with a specific energy of about 120 MJ/kg, which is higher than gasoline (45 MJ/kg), natural gas (50 MJ/kg), and methanol (20 MJ/kg). However, its very low molecular mass (2.016 g/mol for H_2) results in a relatively low volumetric energy density, approximately 10.8 MJ/m³ under standard conditions, compared to natural gas (39.77 MJ/m³) and methanol (16 MJ/m³) [11]. This low volumetric density represents a major challenge for storage and transportation, whether in vehicle applications or pipeline transport. Therefore, acceptable volumetric density is achieved only under high pressure (up to 700 bar) or through liquefaction at extremely low temperatures [7].

Thanks to its high gravimetric energy density and the fact that its combustion produces only water, hydrogen is now considered one of the most promising energy carriers in low-carbon clean energy systems, if challenges related to production, storage, and infrastructure are properly addressed.

1.3 Hydrogen production

Hydrogen can be produced from several different sources. However, currently, hydrogen is mainly produced from hydrocarbon reforming. The choice of hydrogen production process depends on numerous criteria: type of available primary energy, purity, flow rates, etc.…Therefore, hydrogen can be classified according to its production method and sources, with different colors indicating its environmental impact such as:

- **Gray hydrogen:** Produced from fossil sources, without carbon capture.
- **Blue hydrogen:** Produced from fossil sources with carbon capture.
- **Green hydrogen:** Produced from water electrolysis using from renewable sources.

The main current production methods are:

- Hydrogen Production from Fossil Fuels: such as; i) Steam Methane Reforming; ii) Partial Oxidation; iii) Auto thermal Reforming.
- Water Electrolysis.
- Biomass Gasification.
- Coal Gasification.
- Photobiology.
- Hydrogen Production from Nuclear Energy.

1.5 Hydrogen transport

Hydrogen transport technologies must be compatible with its properties and conditions of use:

1.5.1 In the gaseous state: Transporting hydrogen in its gaseous state is one of the most common methods.

1.5.2 In the liquid state: hydrogen can be transported by:

a **Road:** Transporting liquid hydrogen by truck is common for supplying industrial customers.

b **Sea:** from areas with high production capacity to those with high consumption.

1.6 Hydrogen storage

Storage is one of the technological challenges for using hydrogen as an energy carrier. It must provide both a high degree of safety and ease of use in terms of storage capacity and storage/release dynamics to allow different applications to operate under acceptable technical conditions.

Hydrogen can be stored in three different ways: in gaseous, liquid, or solid form. These three storage methods differ in their volumetric and gravimetric densities, as well as in their safety aspects and costs.

1.6.1 Storage under pressure (Gaseous State)

Storage under pressure is one of the most widely used methods currently. Hydrogen can be stored at ambient temperature and under pressure; it is then in a gaseous state and has a low density. For example, at 350 bar, it is 23.66 $kg.m^{-3}$, which corresponds to 933 kWh [6]. The advantage of storing hydrogen under pressure lies in the fact that the technology is highly controlled and filling is very rapid. At the same time, the main drawbacks of this technique are: (i) its low volumetric density; (ii) for high-pressure storage, the adaptation of auxiliary equipment: valves, sensors, pressure regulators, etc.

1.6.2 Liquid storage

Hydrogen liquefies below 20 K at atmospheric pressure. Under these conditions, the liquid is 800 times denser than the gas at ambient temperature, and depending on the type of cryogenic tank used, a specific gravity of around 6.5% is obtained for the complete system. However, this storage method requires a large amount of energy for cooling (25% of the hydrogen combustion energy).

1.6.3 Solid storage

Certain elements have the property of forming bonds (covalent or ionic) with hydrogen, thus enabling its storage, as the phenomenon is reversible under certain operating conditions. These compounds (hydrides), obtained by direct reactions of certain metals or metal alloys with hydrogen, are capable of absorbing hydrogen and releasing it when needed. These materials have been extensively studied for several years, and the selection criteria for a metal hydride for hydrogen storage naturally depend on the intended application (mobile, transportation, portable object, etc., stationary or fixed) and its environment (thermal, etc.). In addition to that, these materials (hydrides) must possess a high specific absorption capacity and rapid absorption/desorption kinetics.

1.6.3.1 Hydrides

Hydrogen sponges, also known as hydrides, are alloys capable of spontaneously absorbing hydrogen, which is then released upon heating. Most metallic elements form hydrides, but the most suitable materials for hydrogen storage must meet the following criteria:

- High absorption capacity of the alloy.
- Low equilibrium pressure at temperatures close to ambient.
- Low exothermic enthalpy of formation.
- Rapid reaction rate, as a slower reaction leads to incomplete hydrogen loading and thus reduced storage capacity.
- Good resistance to aging.
- Moderate cost of the metal or alloy used.

In the following, we will present the different types (classes) of these hydrides and their characteristics as well as the state of the art of research in this field.

a). Metal hydrides

Metal hydrides are represented by the general formula MH_x, where **M** is the metal and **x** is the amount of hydrogen absorbed [6].

The formation of metallic hydrogen begins when hydrogen gas comes into contact with the surface of the metal. At this stage, the hydrogen molecules dissociate into individual H atoms. These atoms then spread within the crystal lattice of the metal and settle in the interstitial spaces between the atoms. This process is characterized by being reversible; the material can absorb hydrogen and release it again when the pressure or temperature conditions change.

b). Alkali metal hydrides

The alkali metals (LiH, NaH, KH, RbH, and CsH) are light, low-density elements that crystallize in a body-centered cubic (BCC) structure, but the density of hydrides is even lower.

c). Alkaline Earth Metal Hydrides

Alkali earth metal hydrides are an important class of hydrides, including elements such as (Be, Mg, Ca, Sr, Ba) with the formula (AeH_2) [6].

d). Magnesium-based metal hydrides

Magnesium (Mg) is one of the most attractive metals for solid-state hydrogen storage due to its light, low density, and abundant natural occurrence, making it suitable for energy applications. Magnesium hydride (MgH_2) is one of the most studied materials in this field because of its high hydrogen storage capacity of approximately 7.6% by weight, as well as its good bulk density of hydrogen [6].

Despite these advantages, MgH_2 faces several challenges that limit its practical use. It requires relatively high temperatures, (285 - 300 °C) ($\Delta H = 75Kj/mol$), to release hydrogen [9]. It also suffers from slow adsorption and decomposition kinetics, in addition to its high thermal stability, which makes hydrogen release less efficient under moderate operating conditions [9].

e) Intermetallic families and their hydrides

Intermetallic compounds are classified according to their chemical structure within the A_mB_n type [6]. Element A is usually a metal capable of readily forming hydrides and is typically a rare-earth or transition element, while element B is a metal that does not readily form hydrides and is a transition element. The resulting hydride is expressed in the general formula $A_mB_nH_x$ [6]: AB family, The AB_2 family, The A_2B family and finally The AB_3 family, which is the least common family and is derived between the AB_2 and AB_5 families. It is characterized by diverse interstitial sites [6].

1.7 Modeling of hydrides within the framework of DFT theory

Calculating the electronic structure of molecules and solids is a discipline that emerged in the last century and has continued to develop rapidly over the past forty years, in parallel with the development of computer science and computational techniques [6]. Many theoretical physicists and chemists have contributed to this growth, from the advent of quantum mechanics to W. Kohn's Nobel Prize in Chemistry in 1998. The starting point for all these developments is the Schrödinger equation, which is known to generally only be solved numerically [6]. To do so, several methods exist, including those based on the first principle or *ab-initio*. Unlike empirical (or semi-empirical) methods, ab initio calculations do not require parameter adjustments to adapt theoretical predictions to experimental results. This does not mean that these methods are perfectly accurate; they rely on a number of approximations that are more or less controlled depending on the case. In first-principles calculations, the key quantity is the energy of the ground electronic state for a given geometry. Precise knowledge of the total energy allows us to deduce other properties of the system under study [6].

Among the ab initio methods, density functional theory (DFT) is particularly important. It consists of reformulating the N-body quantum problem into a problem focusing solely on the electron density.

2 Chapter 2

2.1 Introduction

Hydrogen is an essential element of strategies for transitioning to a green economy, due to its natural abundance, its desired positive environmental impact, and its potential use for decarbonizing industries and transport [8]. However, although hydrogen has considerable potential as an energy carrier, several obstacles can hinder its widespread use, such as the problem of storage.

However, although hydrogen has considerable potential as an energy carrier, several obstacles can hinder its widespread use, such as the problem of storage. Indeed, hydrogen, under normal conditions, occupies an enormous volume for its small mass due to its low density. To circumvent this problem, several methods can be used to store hydrogen, such as high-pressure (up to 700 bars) techniques or cryogenic storage method (at 20 K). However, as mentioned in the previous chapter, these latter methods have some disadvantages such as security and technological problems. It turns out that another solution can overcome these problems. Indeed, solid-state hydrogen storage materials would appear to be the most encouraging solution that can conveniently substitutes to liquefied hydrogen (H_2), with more storage capability and a suitable desorption temperature. This method involves using different types of solid materials that can reversibly store hydrogen and supply it to power the fuel cell.

Among these types of materials, intermetallic alloys have been extensively studied experimentally and theoretically. [9,10,11,12,13], [14]. The intermetallic reversible hydrides are formed from the combination of element A and element B to get the preferred thermodynamic properties [14] and synthesise AB-, AB_2-, AB_3- or AB_5-type alloys for example. These intermetallic alloys have several applications such as thermal applications (cooling system), hydrogen storage switchable mirrors…etc. [14] [15]. For example, AB_3 can be used as negative electrode in Ni-MH batteries or for fuel cell as that, this alloy shows faster reaction kinetics.

Among all AB_3 alloys, Scandium-Based Intermetallic hydrides attracted attention for their physical and chemical properties for applications in solid hydrogen storage [9,10,11,12,13].

This importance stems from structural phase transformations that strongly influence the kinetics of hydrogen absorption and release in these hydrides. Indeed, in scandium-based compounds, their transformations involve unusual bonds and modifications to the crystal lattice that can either facilitate or hinder diffusion and reversibility. [16,17,18].

Within these compounds, Scandium-Palladium system is an intermetallic compound of rare earth elements that have extensively studied theoretically and experimentally [9-13]. These systems are composed of two metals: scandium, which is a light transition metal, and palladium, which is known for its catalytic properties and strong reaction with hydrogen. In this context, $ScPd_3$ has emerged as one of the important intermetallic compounds that has received attention. Three researchers Dwight, Downey and Conner [10] conducted the first study of crystal structure data of $ScPd_3$ (within fifteen AB_3 compounds studied). They used the Nelson-Riley extrapolation to found that $ScPd_3$ has a cubic Cu_3Au-structure (L_{I2}, space group *Pm3m*) with a lattice parameter equal to 3.981 Å [10]. The compound crystallizes in an ideal crystal structure that belongs to the face-centered cubic lattice, which is characterized by a high degree of regularity and structural stability [10]. 12 years later, Erdmann et al [25] confirm the same structure of $ScPd_3$ with an experimental lattice parameter of 3.969 Å.

Several theoretical studies have been conducted to investigate the physical properties of $ScPd_3$ [9,11,12,13], [19].

In fact, Jeong [13] studied the electronic structure and magnetic properties of $ScPd_3$ based on the density functional theory (DFT) through the application of the full-potential nonorthogonal local orbital minimum-basis (FPLO) scheme within the local density approximation (LDA). He found that Sc-3d and Pd-4d states play dominant roles near the Fermi level, in the band structure of $ScPd_3$. He showed that $ScPd_3$ has a stable paramagnetic (non-magnetic) state [13].

Likewise, Khan et al. [19] have calculated the electronic structure of $ScPd_3$ in the framework of DFT using the linearized muffin-tin orbital (LMTO) method. They calculated the intensities of the X-ray emission spectra, considering the transition probabilities and the partial densities of states [19]. Similarly, Lu et al. [20] have calculated the total energies of $ScPd_3$ in the L_{12} structure using the DFT thanks to the full potential and linearized augmented plane waves (FP-LAPW) method [20].

Arikan et al. [11] have investigated the structural, elastic, electronic and phonon properties of $ScPd_3$ compound within DFT using the Quantum-Espresso code. They calculated the elastic constants (C_{11}, C_{12} and C_{44}) in $L1_2$ phase for $ScPd_3$ using the energy-strain method. They showed that this compound is mechanically stable and ductile [11]. They predicted $ScPd_3$ is metal. The specific heat at constant volume was also calculated and discussed using the quasi harmonic approximation [11].

However, Boulechfar et al. [12] studied the mechanical, electronic and thermodynamic properties of $ScPd_3$ in two different structures (LI_2 and D024) using the Full Potential Linearized Augmented Plane Wave (FP-LAPW) formalism. The authors calculated the formation enthalpy and the cohesive energy and concluded that the L_{I2} structure is more stable than the D024 one. Boulechfar et al [12] stated the presence of the pseudo-gap near the Fermi level and they suggested the formation of directional covalent bonding.

Chen et al [8] did a similar work but the $ScPd_3$ was investigated under pressure (between 0 and 50GPa). Indeed, Chen et al [9] studied the structural, elastic, electronic and thermodynamic properties of $ScPd_3$ using pseudopotential method based on DFT under pressure. They found that the bulk modulus (B), shear modulus (G) and Young's modulus (E) for $ScPd_3$ increase with the increasing external pressure.

Although the structural, mechanical, dynamic and thermodynamic properties of the $ScPd_3$ compound were widely studied, its interaction with hydrogen, to our humble knowledge, had never been studied. We found only one experimental work that reported the synthesis of a $ScPd_3$-hydrogen system [21]. Indeed, Latroche et al [21] in their research on the Mg-Sc-Pd-hydrogen system, found by X ray-diffraction a cubic (*Pm-3m*) secondary phase $ScPd_3H_4$ with a lattice parameter of 4.092(4) Å.

Apart from this study, we have no experimental or theoretical work that has highlighted the effect of hydrogen insertion into the ScPd3 matrix. It is essential to elucidate and study the fundamental properties of the hydride in this material in order to explore its potential application in solid hydrogen storage.

This can be done by applying theoretical tools from materials physics such Density functional theory [22-24]. Indeed, the application of DFT can help expand our understanding of the nature of this compound, particularly for subsequent studies related to hydrogen incorporation, providing valuable scientific information that can be used for future development and potential storage of hydrogen.

In this work, we present the results of our study of both $ScPd_3$ and its hydride $ScPd_3H_4$ using first-principles calculations within density functional theory (DFT). This study includes an analysis of the interfacial properties, electronic structure, elastic and mechanical properties of the compound and its hydride, in order to understand their behavior in depth and evaluate the possibility of using the compound in hydrogen storage.

2.2 Computational Method

For this study, the density functional theory (DFT) was used for the intermetallic compound $ScPd_3$ and its hydride $ScPd_3H_4$. Calculations were performed using the CASTEP program.

All of the calculations presented in the manuscript were performed using a digital modelling code called CASTEP (Cambridge Serial Total Energy Package) as a part of a set of digital simulation software called Materials Studio (MS) and marketed by Dassault Systems Biovia. CASTEP is developed in the Condensed Matter Theory group at the University of Cambridge (UK) and was originally generated in 1988 by Payne et al. [22].

CASTEP is an advanced computational program based on quantum mechanics that employs density functional theory (DFT) [23,24], using the plane-wave pseudopotential approach, enabling first principles calculation to simulate the properties of a wide range of materials and solids such as semiconductors, metal, ceramics and zeolites. It can predict properties including elastic constants, structural properties, energy band diagrams, electronic state densities, charge densities and optical properties as well as vibrational and thermodynamic properties. Furthermore, CASTEP provides powerful analysis tools to interpret the calculated results, including electronic structure analysis (band structure and density of states), charge density distribution, optical properties, and mechanical behavior (the bulk modulus, Poisson ratio and Lamé parametres), allowing a deeper understanding of the physical properties of materials.

Briefly, we start our calculation firstly with the construction of the crystallographic structure of our compound ($ScPd_3$ and $ScPd_3H_4$) in our case (figure 1 (left)). Then, we open CASTEP Calculation dialog (figure 1 (right)) to set up and run the calculation. In this box, we can choose the proprieties of our calculation: cut-off energy, k-point sampling, convergence tolerances etc. Indeed, CASTEP code is used to simulate the total energy by special integration of the points in the first Brillouin zone (k-point) with a plane wave base for the expansion of the wave functions (cut-off energy) and the summation in this zone carried out on the vectors of waves produced. These parameters are mandatory and must be carefully study to reach convergence of our calculations. After convergence study, we perform a geometry optimization to obtain reliable results and determine the most stable configuration of the periodic system. This process is achieved through an iterative procedure in which the atomic positions and, if necessary, the lattice parameters are gradually adjusted to minimize the total energy of the system. The optimization continues until the forces and stresses acting on the system reach predefined convergence criteria, resulting in a stable equilibrium structure.

The reference electron configurations are: Sc: $3d^1$ $4s^2$; Pd: $4d^{10}$ and H: $1s^1$. A cutoff energy of 900 eV was used for the plane wave of $ScPd_3$ and its hydride, $ScPd_3H_4$, to ensure good overall energy convergence. The Brillouin zone was sampled using a 12×12×12 k-dot grid. Calculations allowed us to plot convergence curves, which remained stable after adjustment to these values.

The convergence parameters were set at 10^{-6} eV for the overall energy and 0.03 eV/angstrom for the maximum atomic force.

The initial lattice constant was derived from previous experimental data [9] for $ScPd_3$ (a = 3.981 angstroms).

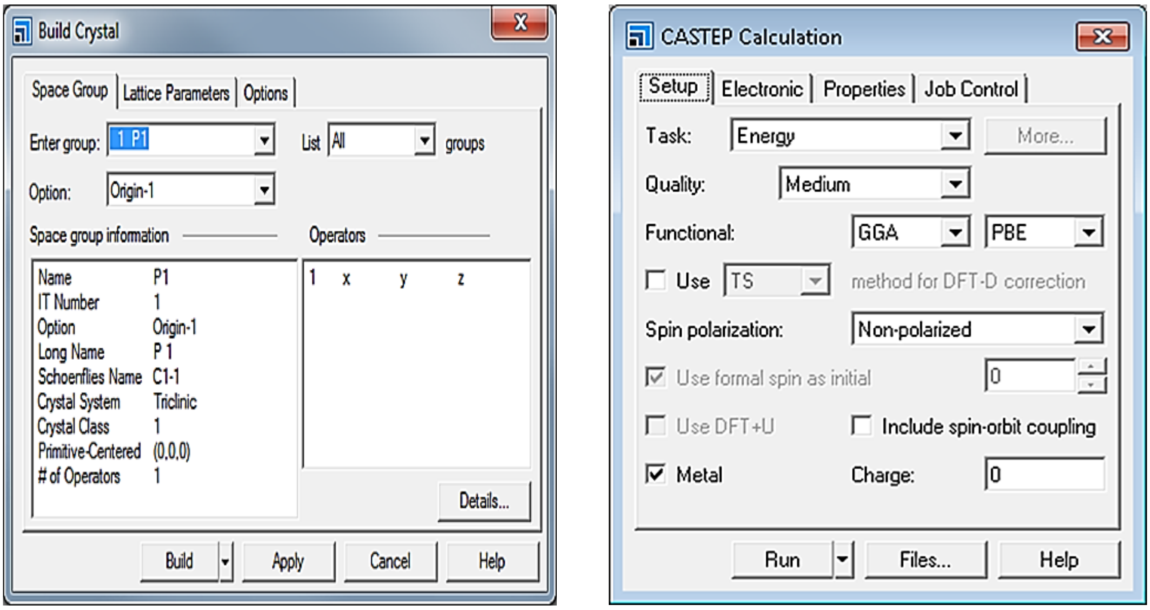

Enter group: 1 P1

List: All groups

Option: Origin-1

Space group information

Name	P1
IT Number	1
Option	Origin-1
Long Name	P 1
Schoenflies Name	C1-1
Crystal System	Triclinic
Crystal Class	1
Primitive-Centered	(0,0,0)
# of Operators	1

Operators

1 x y z

Task: Energy

Quality: Medium

Functional: GGA PBE

☐ Use TS method for DFT-D correction

Spin polarization: Non-polarized

☑ Use formal spin as initial 0

☐ Use DFT+U

☐ Include spin-orbit coupling

☑ Metal

Charge: 0

Figure 2-3: CASTEP windows interfaces of: crystal structure input (left) and CASTEP calculation parameters (right).

2.3Results and Discussion

2.3.1 Structure properties

The $ScPd_3$ compound adopts a regular cubic $L1_2$, (Cu_3Au-Type) structure with a Pm-3m space group (n° 221) as illustrated in figure 2.

Indeed, the scandium atom occupies the corners of the cell at coordinates (0,0,0) with (*1a* site), while the three palladium atoms occupy the face-center positions at coordinates (1/2,1/2,0) (*3c* site). The experimental lattice parameter and atomic Wyckoff positions are reported in Table 1.

The $ScPd_3H_4$ hydride have the same crystallographic structure space group: regular cubic $L1_2$, (Cu_3Au-Type) structure with a Pm-3m space group (n° 221) see figure 3.

Maintains its structure and composition, as the hydrogen atom H (1) occupies the center of the cell at coordinates (1/2,1/2,0), and the hydrogen atom H (2) is also positioned in the octa hydric sites within the crystal lattice at coordinates (0,0,1/2).

The lattice constant value at equilibrium was calculated to be 4.009Å (After structural relaxation, the optimal lattice constant was found exactly to be 4.00959 angstroms). Table.1 shows the calculated values based on the Density Function Theory (DFT) for $ScPd_3$, along with the available experimental and theoretical values. $ScPd_3H_4$ hydride is obtained by inserting hydrogen atoms into the interstitial positions within the crystal lattice, as shown in (Fig.2). We observe that it retains the cubic structure. It is clear from the table that our current results and the available data show that the lattice constant of the hydride is greater than that of the original compound. This allows us to understand that an expansion of the crystal cell size occurred without significant asymmetry. It retained its cubic structure, which indicates an important property and suggests that it is an excellent candidate for hydrogen storage.

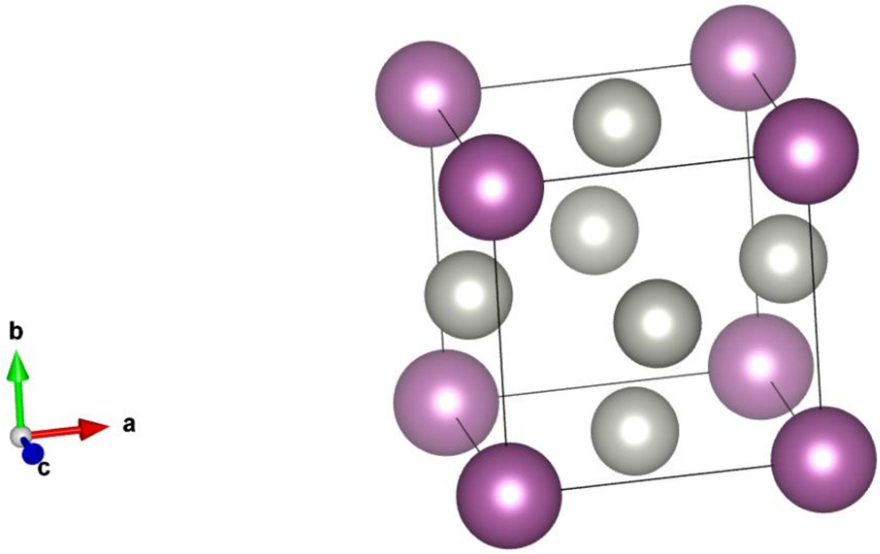

Figure 2-4: Crystal structure of $ScPd_3$ compounds in the $L1_2$. Big (purple) and small(gray) ball are Sc and Pd atoms, respectively.

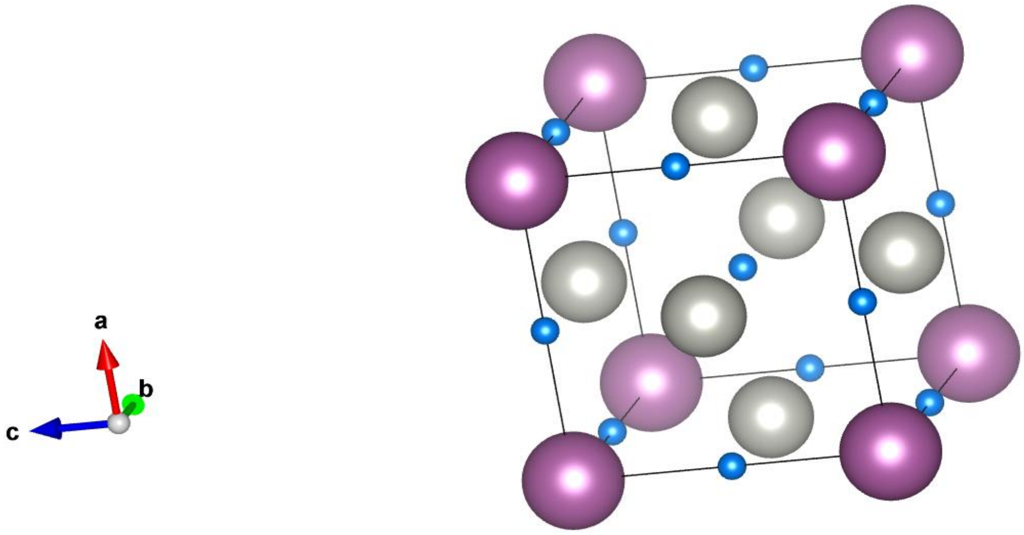

Figure 2-5 :Crystal structure of $ScPd_3H_4$ compounds in the $L1_2$ Big (purple) small (gray) and smaller (blue) ball are Sc, Pd and H atoms respectively.

Table 2-1 The crystal structure of the compound $ScPd_3$ and its hydride $ScPd_3H_4$ (space group Pm-3m) was determined. Position occupancy factors 1a, 1b, and 1c were defined as constraints.

	Space Groupe	**Wyckoff**	**Element**	**x**	**y**	**z**	***a*** **(Å)**		**Molar Mass(g/mol)**
$ScPd_3$	Pm-3m n° (221)	1a	Sc	0	0	0	This work	4.010	364,228
		3c	Pd	1/2	1/2	0	Theo [4]	4.015	
		1a	Sc	0	0	0	Theo [2]	3.989	
							Exp [3]	3.981	
$ScPd_3H_4$	Pm-3m n° (221)	1b	H	1/2	1/2	1/2	This work	4.21	368,252
		3c	Pd	0	1/2	1/2	Exp [14]	4.092	
		3d	H	1/2	0	0			

The relative deviation between theoretical and experimental values is approximately 0.72% for $ScPd_3$, while its hydride, $ScPd_3H_4$, has a percentage of 3%, indicating an excellent agreement and confirming the reliability of the computational setup.

We observe an increase in the crystal lattice constant from 4.01Å for the compound $ScPd_3$ to 4.21Å for its hydride $ScPd_3H_4$. This indicates an expansion of the volume of the crystal structure of the compound after the introduction of hydrogen, as the compound increased by 15% (measuring the effect of hydrogen introduction).

This result confirms that hydrogen is the cause of a clear expansion in the structure of the compound.

2.3.2 Elastic properties

The elastic constants are among the most important parameters used to describe a material's strength and rigidity under external pressure. They assess compressive strength and mechanical stability, thus helping to understand the mechanical behavior of materials. In the cubic crystal system only three independent materials (C_{11}, C_{12}, C_{44}) describe these properties. In our case, since the compound $ScPd_3$ and its hydride $ScPd_3H_4$ both have a cubic structure, these three elastic constants exhibit different values and reported in Table - 2. We can observe that the calculated values for $ScPd_3$ are almost identical to the other theoretical values [8,11-12], but, no experimental values are found in the literature. Moreover, and in the best of our knowledge there are no experimental or theoretical data for elastic constants of $ScPd_3H_4$. The mechanical stability criteria [10-11] for cubic structure are:

$$C_{11} > 0 \; ; C_{12} > 0 \; ; C_{11}-C_{12} > 0 \; ; \; C_{11}+2C_{12} > 0$$

From table 2, the criteria are satisfied which means that these materials are mechanically stable.

Table 2-2 :Calculated elastic constants (GPa) and derived mechanical properties of $ScPd_3$ and $ScPd_3H_4$.

	Reference	***C_{11}***	***C_{12}***	***C_{44}***	***B***	***G***	***E***
$ScPd_3$	This work	182.65	114.57	76.01	137.26	55.06	145.71
	Theor [4]	207.35	120.29	84.42	164.20	68.06	177.26
	Theo [2]	197.77	128.17	88.99	151.37	61.07	161.50
	Theo [5]	180.99	126.11	84.04	144.40	53.73	143.40
$ScPd_3H_4$	This work	158.64	123.50	54.02	135.21	34.48	95.33

The compound and its hydride met the mechanical stability requirements of the cubic system. However, the introduction of hydrogen into the compound led to a decrease in the elastic constants C_{11} and C_{44}, indicating a decrease in the material's stiffness and an increase in its deformability. The volumetric compressive modulus B and the shear modulus G were calculated based on the elastic constants C_{11}, C_{12}, and C_{44}. Young's modulus E was calculated based on the volumetric compressive modulus B and the shear modulus G. The results showed that the value of E decreased significantly after the introduction of hydrogen, reflecting a decrease in the overall stiffness of the material. This decrease is directly related to the decrease in the shear modulus G, while the volumetric compressive modulus B remained nearly constant.

2.3.3 Electronic properties

Density of States (DOS) and electronic band structure analysis is essential for understanding the electronic and bonding properties of both $ScPd_3$ and $ScPd_3H_4$ intermetallic compound. Furthermore, the electronic band structure along the high-symmetry directions of the Brillouin zone was evaluated to investigate the electronic properties and confirm the metallic nature of the $ScPd_3$ and $ScPd_3H_4$ compound (Fig.4). To gain a deeper understanding of the bonding nature, both the Total DOS and Partial DOS were calculated and shown in (Fig.5).

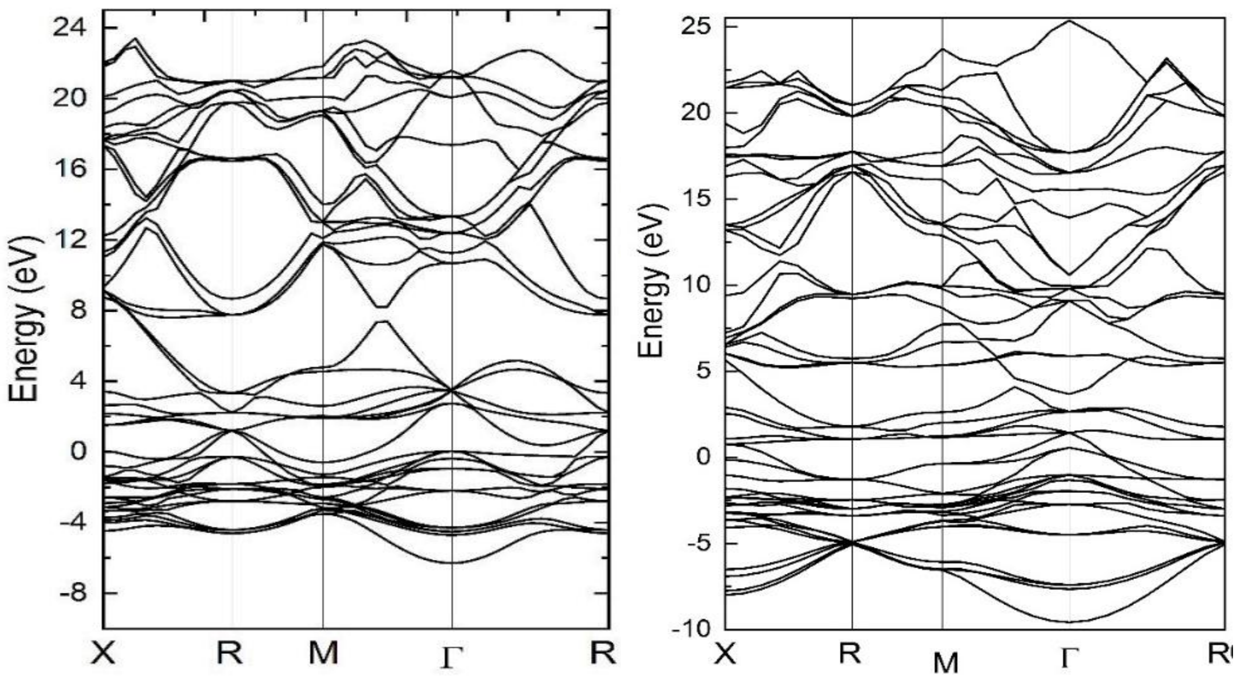

Figure 2-6 : Electronic band structure of $ScPd_3$ and $ScPd_3H_4$ along the high- symmetry directions

Analyzing the band structure curve of $ScPd_3$ reveals that it spans an energy range of -8 eV to -24 eV. A high band density and numerous overlapping electron bands are observed between -4 eV and 0 eV, particularly at the 0-eV level. This filled level is known as the Fermi level. From this, we conclude that the compound is a good conductor at 0 eV. Overlap is also observed along the band structure itself. These observations lead us to conclude that the compound exhibits excellent metallic properties. Similarly, for hydrogen insertion ($ScPd_3H_4$), we observe an energy range of -10 eV to -24 eV and numerous overlapping electron bands at 0 eV, also known as the Fermi level, indicating its metallic nature. The band density is found to range between -5 eV and 0 eV. We also note that after the introduction of hydrogen to the electrons in their electron orbitals, there were fluctuations in energy at the level of each band structure curve of the hydride compound. Therefore, even with the addition of hydrogen, its metallic properties remain unchanged, indicating a change in the orbital levels of the scandium and palladium atoms.

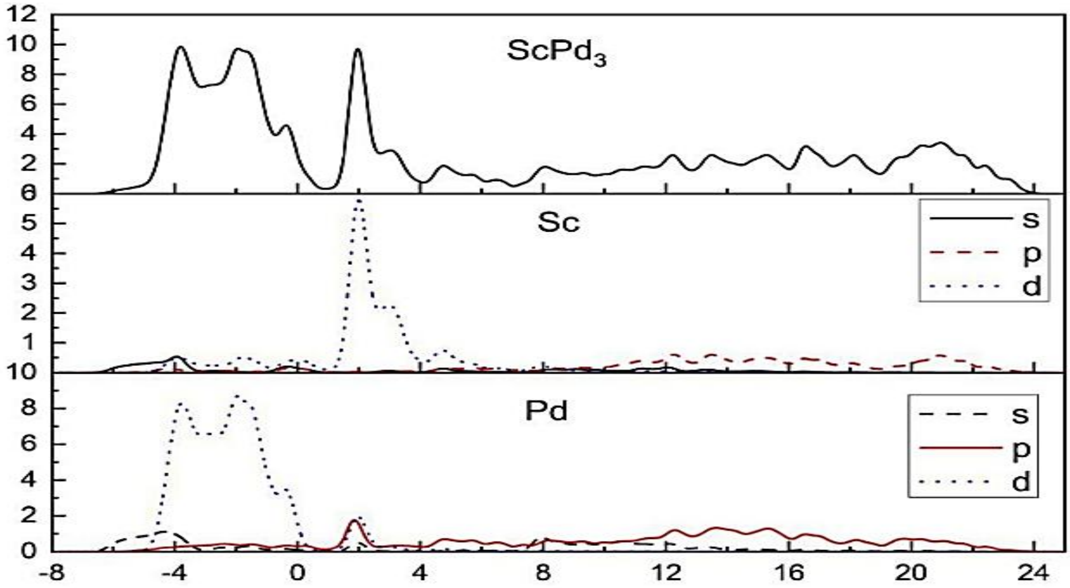

Figure 2-7 : The partial and total density of states of $ScPd_3$

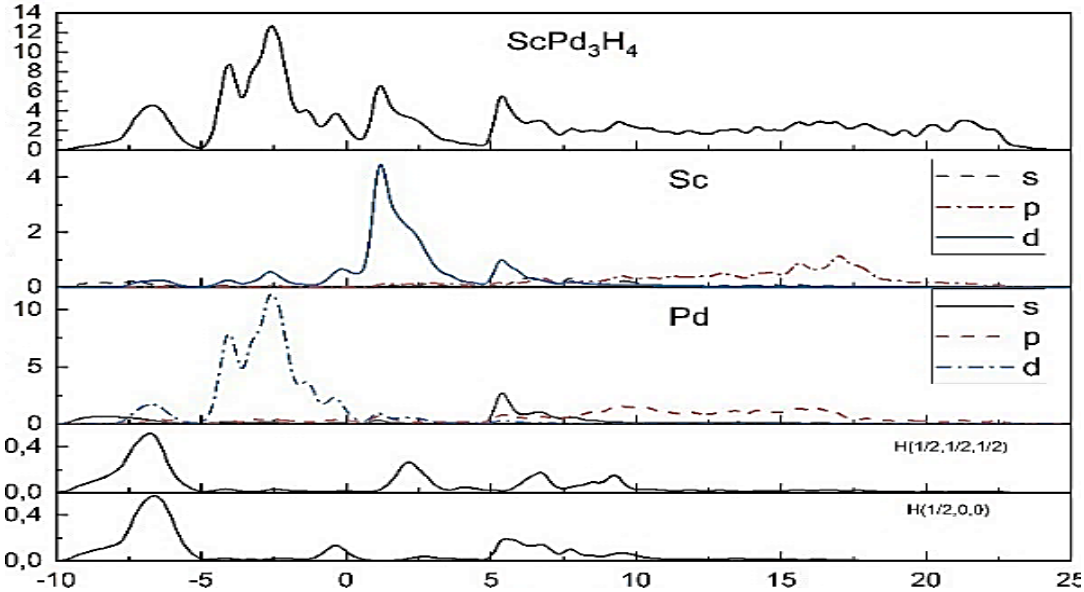

Figure 2-8 : The partial and total density of states of $ScPd_3H_4$

By analyzing the partial density of states (PDOS) and total density of states (TDOS) diagrams shown in Figure 5, and based on the electron orbitals of both the compound $ScPd_3$ and its hydride $ScPd_3H_4$, we can see that the scandium electron orbitals in $ScPd_3$ are less prominent than those of palladium, which initially appear strongly. This indicates that palladium is the primary contributor to the metallic character. Furthermore, overlap between the two atoms in certain orbitals is observed, facilitating our understanding of the compound's nature. We conclude that the Pd-d electrons dominate, with a weak contribution from Sc. In the hydride $ScPd_3H_4$, we observe that the palladium atom, after the addition of hydrogen, is the first electron to react with another palladium atom. The curves also show that the main contributions are made by the Pd-d, Sc-d, and H-s orbitals. Therefore, it is clear that palladium is the dominant element, scandium is a secondary element, and hydrogen contributes to modifying the bonding structure.

2.3.4 Optical properties

This section studies the optical properties of the compound $ScPd_3$ and its hydride $ScPd_3H_4$ through several optical parameters including the dielectric function, loss function, refractive index, absorption, conductivity, and reflectivity. The density functional Perturbated Theory (DFPT) is used to calculate all these optical properties. The dielectric function can be expressed as follow:

$$\varepsilon(\omega)=\varepsilon_1(\omega)+i\varepsilon_2(\omega) \qquad (3)$$

where $\varepsilon_1(\omega)$ is the real part and $\varepsilon_2(\omega)$ is the imaginary part. Some of the remaining properties are described and derived from the dielectric function. Consequently, we report the reflectivity, absorption, dielectric function, refractive index, conductivity, and loss functions of $ScPd_3$ and $ScPd_3H_4$ in fig.7 and 8, respectively.

In the following, we analysis all the optical parameters cited previously. This analysis offers valuable new insights into the scientific studies of the optical behavior of $ScPd_3$ in general, and $ScPd_3H_4$ primarily a new description of its applications in optoelectronic device.

The real part ε1 (Re(ε)) of the compound $ScPd_3$ initially appears at 0 eV with is a high positive value. Then, gradually decreases until it crosses zero around 4 eV to reach the lowest value at 5 eV and finally vanished after 20 eV. When the real part becomes negative to positive (in our case ~4 eV) i.e., a material with a metallic behavior at a high photonic energy value, the material moves from a reflective material to a transparent material. This point represents the plasma frequency. At the same energy, the imaginary part ε2 (Im (ε)) shows a clear positive peak (~4 eV).

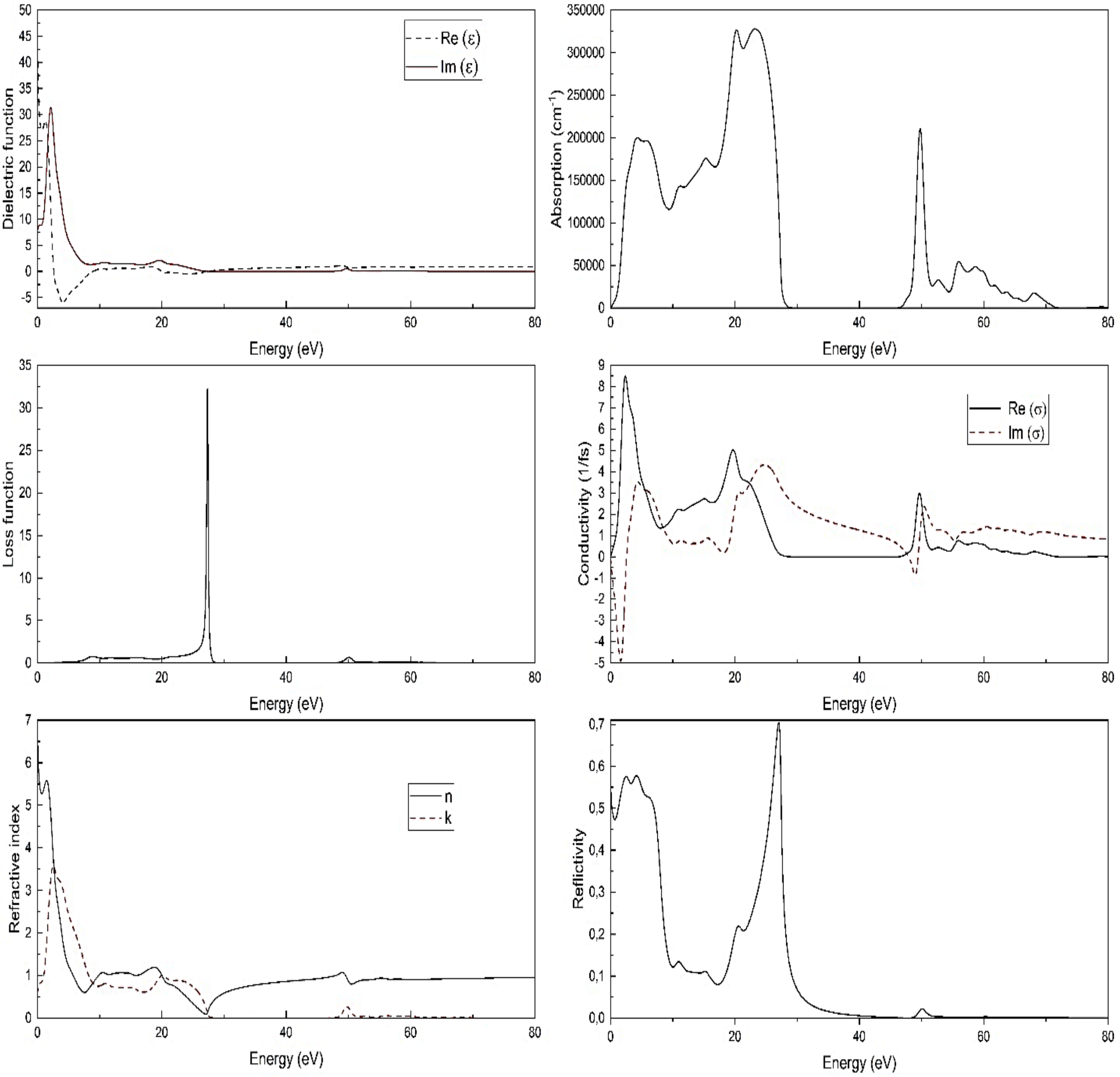

Figure 2-9 : The optical functions (a) reflectivity, (b) absorption, (c) dielectric function, (d) refractive index, (e) conductivity, and (f) loss function of $ScPd_3$ intermetallic compound

As shown in the Absorption curve of the compound $ScPd_3$, where absorption starts from a photon energy of zero, the value of the absorption intensity, which represents a high value (from 5×10^4 to 35×10^4 cm^{-1}), indicates the compound's high ability to absorb electromagnetic ignition, making it suitable for a specific optical application. The large increase in the absorption coefficient confirms the metallic nature of the compound $ScPd_3$.

$$\delta = \frac{1}{\alpha} \qquad (4)$$

$$\delta = \frac{1}{35\times10^4} = 2{,}85\times10^{-6}cm$$

The refractive index curve n(ω) shows relatively high values, indicating a strong interaction between light and matter. It starts at 6, and gradually slows down until to be near 1 at 7.5 eV. The refractive index n is related to the speed of light, where n = c/υ, where c is the speed of light in a vacuum and v is the speed of light inside matter. Therefore, υ = c/n. Thus, if n is large, light travels slower in matter, and if n is small, light travels faster. When comparing the values from the curve, n is approximately equal to 5.6. Therefore, the speed of light in this material is estimated at 5×10^7 m/s, which is one-fifth of the speed of light in a vacuum (3×10^8 m/s). This indicates a slowdown in the speed of light propagation compared the propagation in vacuum.

The refractive index of the compound $ScPd_3$, n=5.6, is considered high compared to other materials. Indeed, the refractive index of air n_{air} = 1.0003 and semiconductor values often n= 2-4, the compound's very high refractive index indicates a strong electron response. The higher the n value, the greater the effect on light. This suggests a strong interaction between light and matter. For example, using Snell's Law,

$$n_{\text{air}} sin\theta_1 = n_{\text{ScPd3}} sin\theta_2 \qquad (5)$$

We can estimate the probability of light striking at an angle of θ_1=30° to be:

$$1\sin30 = 5\sin\theta_2$$

$$0.5 = 5 sin\theta_2$$

$$sin\theta_2 = 0.1$$

$$\theta_2 = 5{,}7°$$

We see that the angle of incidence is determined by the angle of refraction. This is considered a large curvature, and all of this is due to the large value of n in light. It slows down and is deflected more, so the greater the n, the smaller the angle of curvature.

The reflectivity curve of the $ScPd_3$ compound shows that, between 0 and 30 eV photon energies, its value ranged from 0.5 to 0.7 more precisely. This means that 50% to 70% of the light incident on the compound's surface is reflected instead of being absorbed. This is due to the free electrons in the compound, which create a magnetic field that reflects and refracts the incoming light wave. We also observe a decrease in reflectivity as the photon energy increases, allowing it to be absorbed rather than reflected in this region.

The conductivity curve shows that it consists of a real and an imaginary part, which exhibit a clear difference at the beginning. The real part reaches a maximum value of σ_{max} of 8.5 fs^{-1}, starting from zero. We also observe that it then fluctuates and decreases as the photon energy increases, ranging from 0 to 80eV. The imaginary part also starts from zero, with a minimum value of -5fs^{-1} at 2 eV. We also observe that its conductivity increases with increasing photon energy.

The loss function curve, which represents the loss of electron energy within the material, shows a sharp and strong value at an energy of 27 eV. This is due to the density of free electrons within the compound at that value and point. This value also coincides rapidly with a decrease in the energy limit.

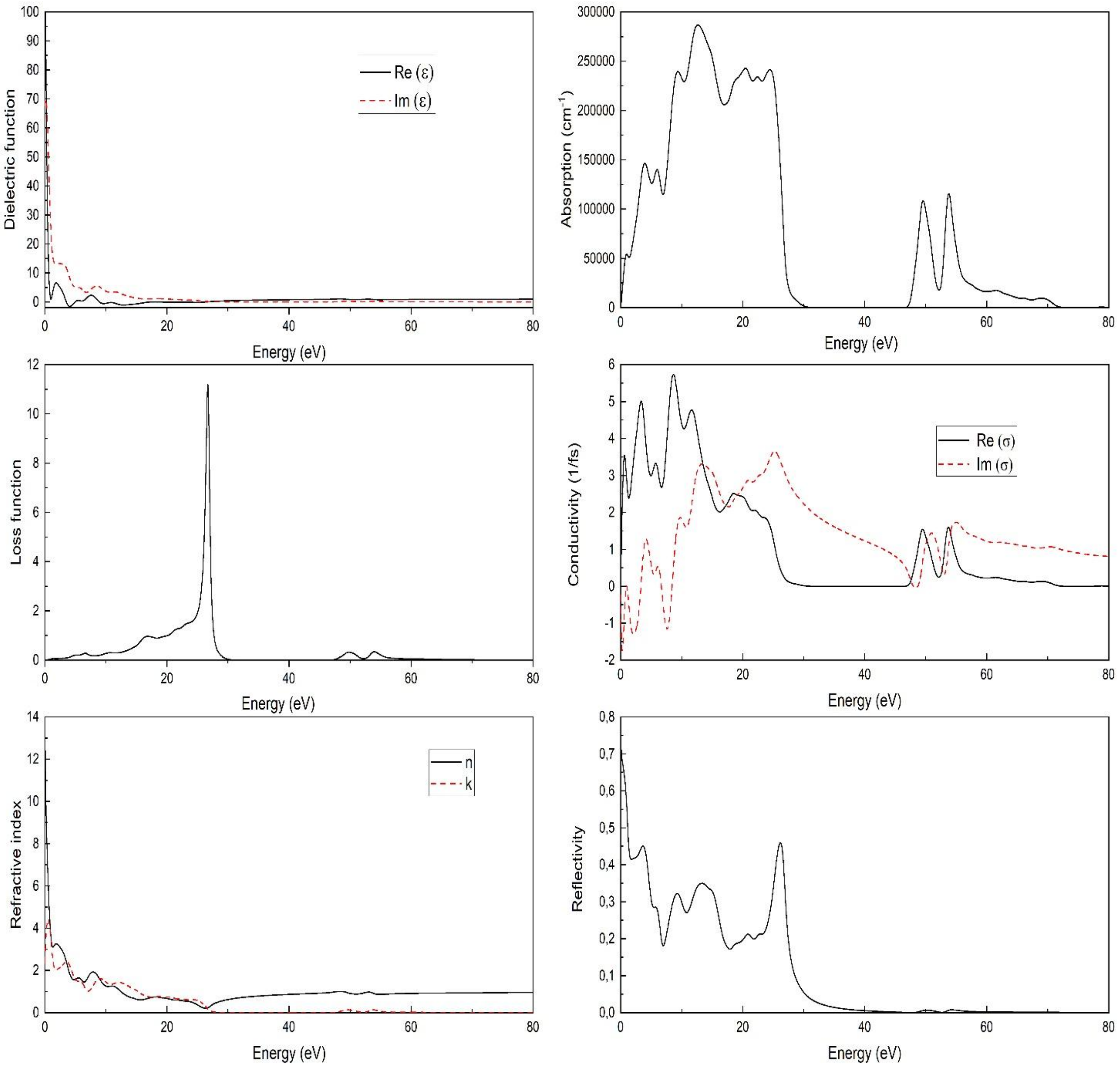

Figure 2-10 : The optical functions (a) reflectivity, (b) absorption, (c) dielectric function, (d) refractive index, (e) conductivity, and (f) loss function of $ScPd_3H_4$ intermetallic compound.

The calculated results show that the hydrogenation of $ScPd_3$ to $ScPd_3H_4$ had a clear effect on the optical response. The dielectric constant ε shows that the real part ε exhibits a very strong hydrogen absorption response, starting with a peak at a stable value of approximately 80. This is a large value compared to some known hydrides, for example, in MgH_2, where the value is between 3.8 and 4.5. This indicates that $ScPd_3H_4$ has a strong polarizability. We also observe a significant decrease in the ε value until vanished over 30 eV photon energy.

The absorption spectrum also reveals that the absorption coefficient reached a value of ($29 \times 10^4 cm^{-1}$ at 12 eV) which is a very high value and similar to $ScPd_3$ one, indicating strong absorption of electromagnetic radiation, especially in the ultraviolet range ($2{,}5000 \times 10^6 cm^{-1}$). The major peak is located within this range. The absorption range α, which reached a very large value, represents the extent to which a material absorbs light. The higher the value of α, the less the depth of penetration of light into the material. According to the relationship, the depth of penetration was:

$$\delta = \frac{1}{29 \times 10^{4}} = 3{,}44\ \times 10^{-6} cm$$

This means that the light was absorbed only in tens of nanometers.

The loss function shows a strong and sharp peak around ~25 eV, reaching a value of approximately 9–10, which represents the maximum energy loss of electrons inside the material. This peak indicates a strong electronic response and confirms the metallic nature of the compound. At lower energies (below 10 eV), the values remain close to zero, indicating weak energy loss in this region.

The optical conductivity starts from very low photon energies (near 0 eV) with noticeable values of about 1–2 fs^{-1}, which indicates that electrons can move easily under the effect of light. Several peaks are observed between ~2 eV and 10 eV, reaching values up to around 5–5.8 fs^{-1}, corresponding to electronic transitions between energy levels. As the photon energy increases beyond 15 eV, the conductivity gradually decreases toward lower values, indicating a reduction in these transitions.

The refractive index shows a high value at low photon energies, starting from approximately 6–7 at 0 eV, which indicates a strong interaction with light. As the energy increases, the refractive index decreases gradually and becomes nearly constant around 1–2 above 20 eV, showing that the interaction between light and the material weakens at higher energies.

The reflectivity exhibits high values at low photon energies, around 0.6–0.7, confirming that the material reflects a significant portion of incident light. A noticeable peak appears between ~20 and 25 eV, reaching values close to 0.45. After this region, the reflectivity decreases significantly toward lower values (below 0.2), indicating reduced reflection at higher photon energies.

Overall, these results confirm that $ScPd_3H_4$ exhibits a metallic optical behavior, characterized by strong electron–photon interaction in the low-energy region and a pronounced plasmon peak at higher energies.

2.4 Hydrogen storage capacity of $ScPd_3H_4$

For the $ScPd_3H_4$ the weight percent of hydrogen was calculated using the ratio of the total hydrogen mass to the total mass of the compound.

The molar mass of $ScPd_3H_4$ was determined by summing the atomic masses of its constituent elements (Sc, Pd, and H), resulting in a total value of 368.25 (g/mol), the contribution of hydrogen corresponds to 4.032 g/mol. Based on these values the hydrogen weight percent was estimated to be approximately 1.09 Wt%

$$\text{Wt\% (H)} = \frac{4 \times 1.008}{44.96 + 3 \times 106.42 + 4 \times 1.008} \times 100 = \frac{4.032}{368.25} \times 100 = 1.09 \text{ wt\%} \qquad (6)$$

This relatively low hydrogen content indicates that, although the compound is structurally stable and capable of incorporation hydrogen its gravimetric hydrogen storage capacity remains limited compared to materials with higher hydrogen content.

2.5 Enthalpy of formation

The enthalpy represents the energy change associated with the formation of the compound from its constituent elements, (ΔH_f) calculate by taking the difference in total energy of the products and reactants [26]

For the $ScPd_3H_4$ system, the enthalpy of formation was calculated according to the next reaction equation:

$$ScPd_3 + 2H_2 \rightleftharpoons ScPd_3H_4 \qquad (7)$$

Accordingly, the enthalpy of formation is given by:

$$\Delta H = E_{tot}(ScPd_3H_4) - [E_{tot}(ScPd_3) + 2E_{tot}(H_2)] \qquad (8)$$

Where $E(ScPd_3H_4)$ is the total energy of the hydrogenated system (table 3), $E(ScPd_3)$ is the total energy of the pristine compound (table 3), Since hydrogen naturally exists as a diatomic molecule (H_2), it cannot be treated as an isolated atom within the density functional theory (DFT) framework. Therefore, the total energy of hydrogen was calculated using an H_2 molecule.

The H_2 molecule was modelled by placing two hydrogen atoms at an initial bond length of approximately 0.74 Å within a big box to eliminate interactions between periodic images. The size of the supercell was carefully chosen to ensure that the total energy remains independent of the vacuum spacing, thus accurately representing an isolated molecule. Geometry optimization was then performed, allowing only the H–H bond length to relax until convergence was achieved. The resulting total energy was taken as the reference energy $E(H_2)$.

Table 2-3: Total energies and enthalpy of formation

H_2 (Energy\eV)	$ScPd_3$ (Energy\eV)	$ScPd_3H_2$ (Energy\eV)	ΔH (Energy\eV)
-31,72151	-10365,2205	-10427,88994	-0,77359

The calculated value of the enthalpy of formation is ΔH= -37,31 KJ/mol.H_2

This negative value indicate that the formation of the hydride is thermodynamically favorable (exothermic reaction), confirming the stability of the hydrogenated structure it also suggests that the incorporation of hydrogen into $ScPd_3$ lattice is energetically advantageous.

Table 2-4: Comparison of enthalpy of formation

Compound	**ΔH_f (kJ/mol H_2)**
MgH_2	-67.8 [27]
$LaNi_5H_2$	-31,6 [28]
$ScPd_3H_4$	-37.31

The comparison of the enthalpy of formation values shows that $LaNi_5H_6$ has a value of −31.6 kJ/mol H_2, indicating moderate hydrogen–metal interaction and good reversibility. MgH_2, on the other hand, exhibits a much more negative value (−67.8 kJ/mol H_2), reflecting strong hydrogen bonding and high thermodynamic stability, but with more difficult hydrogen release. After normalization, the enthalpy of formation of $ScPd_3H_4$ is found to be −37.31 kJ/mol H_2, which lies between the two systems. This indicates that the hydrogen–metal interaction in $ScPd_3H_4$ is stronger than in $LaNi_5H_6$ but significantly weaker than in MgH_2. Such intermediate behavior suggests that $ScPd_3H_4$ may offer a good balance between stability and hydrogen release, making it a potentially promising candidate for hydrogen storage applications.

Conclusion

This work presents a comprehensive study of the effect of hydrogen incorporation on the $ScPd_3$ compound, which is considered a promising material for hydrogen storage and clean energy applications. This research aligns with the growing global interest in developing new materials capable of improving energy storage efficiency, particularly given the trend toward reducing reliance on traditional, polluting energy sources. Using density functional theory (DFT) as implemented in the CASTEP code we study the structural, electronic, mechanical, optical thermodynamic properties of the $ScPd_3$ and $ScPd_3H_4$.

Our calculations show that the geometry optimization confirmed the experimental lattice parameters of these materials and confirm the stability of the studied structures after hydrogen incorporation.

The calculated electronic structure showed that both $ScPd_3$ and $ScPd_3H_4$ exhibit a distinct metallic character, with a high density of electronic states at the Fermi level (0 eV) so the hydrogen insertion has no effect to the chemical bond nature. TDOS and PDOS analyses also revealed that the Pd-d states contribution is dominant in the electronic behaviour, while the Sc-d contribution is less significant. Following hydrogen introduction, a slight redistribution of the density of states was observed involving H-s, Sc-d, and Pd-d orbitals, without altering the metallic nature of the compound.

The calculated optical results showed that $ScPd_3$ exhibits a high refractive index (~6 at 0 eV) that decreases to ~1 at high energies, with reflectance between 0.5 and 0.7 in the 0–30 eV range, and a very high absorption coefficient reaching (5×10^4–35×10^4 cm^{-1}). An energy loss peak was also recorded at ~27 eV and a maximum conductivity value of ~8.5 fs^{-1}. After hydrogenation ($ScPd_3H_4$), the dielectric response increased, with ε reaching ~80, and strong absorption up to ~29×10^4 cm^{-1} at ~12 eV. A loss peak also appeared at ~25 eV with a value of 9–10, and a refractive index of ~6–7 at 0 eV that decreases to ~1–2 at high energies. Reflectivity was ~0.6–0.7 at low energies, with transmission peaks between 2–10 eV reaching ~5.8 fs^{-1}.Overall, the results confirm that both compounds exhibit metallic behaviour, with hydrogen contributing to an increase in certain optical values (polarizability and absorption) while preserving the fundamental properties.

The formation enthalpy (ΔH_f) of the $ScPd_3H_4$ compound was calculated based on the total energy of $ScPd_3$, hydrogen (H_2), and the final compound. We have found the value of this enthalpy is -37.31 $kJ/mol\cdot H_2$ which indicate that the hydride formation process is exothermic (negative value) and thermodynamically favourable, confirming that the incorporation of hydrogen into the $ScPd_3$ lattice occurs in a stable and energetically favourable manner. A comparison between the formation enthalpies of $ScPd_3H_4$ and those of $LaNi_5H_6$ and MgH_2 indicates that $ScPd_3H_4$ has the lower enthalpy, which indicates that the hydrogen can be restituted (reversible formation reaction) easily than in the case of $LaNi_5H_6$ and MgH_2. This is favourable for hydrogen storage applications.

The hydrogen content in $ScPd_3H_4$ was also calculated based on the total molar mass (368.25 g/mol), yielding a hydrogen value of 4.032 g/mol, equivalent to 1.09 wt%. This result indicates that the compound contains a low percentage of hydrogen (the same range of hydrogen content of $LaNi_5H_6$ and $LaNi_5H_2$). This is favourable for stationary hydrogen storage application than mobile hydrogen storage.

As perspective, an experimental study for these materials is mandatory to confirm our theoretical investigation.

Reference

[1]. Khan, K., Khurshid, A., & Cifuentes-Faura, J. (2023). Energy security analysis in a geopolitically volatile world: A causal study. Resources Policy, 83, 103673. https://doi.org/10.1016/j.resourpol.2023.103673

[2]. Goshua, A., Akdis, C. A., & Nadeau, K. C. (2022). World Health Organization Global Air Quality Guideline Recommendations: Executive summary. Allergy, 77(7), 1955–1960. https://doi.org/10.1111/all.15224

[3]. Guan, D. et al. (2023) 'Hydrogen society: From present to future', Energy & Environmental Science, 16(11), pp. 4926–4943.

[4]. Energy Institute. (2025). Statistical Review of World Energy 2025. London: Energy Institute. (See p. 31, Crude Oil Price Curve 1861–2024).

[5]. https://berkeleyearth.org/global-temperature-report-for-2025/ consulted on 12 May 2026

[6]. Bouhadda, Y.2011 Etude des hydrures en vue d'une application pour le stockage de l'hydrogène. Modélisation des propriétés électroniques et thermodynamiques par calcul Ab initio. Université USTHB, N° d'ordre: 12/2011-D/PH

[7]. Atilhan, M., et al. (2021). Hydrogen production, storage, utilisation and environmental impacts: a review. Environmental Chemistry Letters.

[8]. Breyer C., Lopez G., Bogdanov D., Laaksonen P. The role of electricity-based hydrogen in the emerging power-to-X economy Int J Hydrog Energy, 49 (2024), pp. 351-359

[9]. Chen, B., Qi, S., Song, H., Zhang, C., & Shen, J. (2015). First-principle investigations on structural, elastic, electronic and thermodynamic properties of ScX_3 (X = Ir, Pd, Pt and Rh) under high pressure. Modern Physics Letters B, 29(32), 1550201. https://doi.org/10.1142/S0217984915502012

[10]. Dwight, A. E., Downey, J. W., & Conner, R. A., Jr. (1961). Some AB_3 compounds of the transition metals. Acta Crystallographica, 14, 75.

[11]. Arıkan, N., İyigör, A., Candan, A., Uğur, Ş., Charifi, Z., Baaziz, H., & Uğur, G. (2013). Structural, elastic, electronic and phonon properties of scandium-based compounds ScX_3 (X = Ir, Pd, Pt and Rh): An ab initio study. Computational Materials Science, 79, 703–709. https://doi.org/10.1016/j.commatsci.2013.07.041

[12]. boulechfar, R., Trad Khodja, A., Khenioui, Y., Meradji, H., Drablia, S., Chouahda, Z., Ghemid, S., Naqib, S. H., Khenata, R., & Wang, X. T. (2019).First-principle study of the structural, mechanical, electronic and thermodynamic properties of intermetallic compounds: Pd_3M (M = Sc, Y). International Journal of Modern Physics B, 33(27), 1950321. https://doi.org/10.1142/S0217979219503211

[13]. Jeong, T. (2006). First-principles studies on the electronic structure of $ScPd_3$. Solid State Communications, 140, 304–307.

[14]. l Kumar, P. Muthukumar, P. Sharma, E. A Kumar: Absorption based solid state hydrogen storage system: A review. Sustainable Energy Technologies and Assessments 52 (2022) 102204. https://doi.org/10.1016/j.seta.2022.102204.

[15]. W. Liu, C.J. Webb, E.MacA. Gray, Review of hydrogen storage in AB3 alloys targeting stationary fuel cell applications, International Journal of Hydrogen Energy 41 (2016) 3485-3507. https://doi.org/10.1016/j.ijhydene.2015.12.054.

[16]. Yartys, V., Berezovets, V., Vajeeston, P., Akselrud, L., Antonov, V., Fedotov, V., Klenner, S., Pöttgen, R., Chernyshov, D., Heere, M., Senyshyn, A., Denys, R., & Havela, L. (2022). HYDROGEN INDUCED STRUCTURAL PHASE TRANSFORMATION IN ScNiSn-BASED INTERMETALLIC HYDRIDE CHARACTERIZED BY EXPERIMENTAL AND COMPUTATIONAL STUDIES. Acta Materialia. https://doi.org/10.1016/j.actamat.2022.118549

[17]. Yartys, V., Webb, C., & Cuevas, F. (2023). In situ Diffraction Studies of Phase-Structural Transformations in Hydrogen and Energy Storage Materials: an Overview. Journal of Alloys and Compounds. https://doi.org/10.1016/j.jallcom.2023.170133

[18]. Latroche, M. (2010). Structural transitions induced by hydrogen absorption in metallic hydrides., 223, 666 - 673. https://doi.org/10.1524/zkri.2008.1019

[19]. M.A. Khan, C. Koenig, J. Phys. C9 (1987) 1067.

[20]. Z.W. Lu, B.M. Klein, A. Zunger, Phys. Rev. Lett. 75 (1995) 1320.

[21]. Latroche, M., Kalisvaart, P., & Notten, P. H. L. (2006). Crystal structure of $Mg_{0.65}Sc_{0.35}D_x$ deuterides studied by X-ray and neutron powder diffraction. Journal of Solid-State Chemistry, 179, 3024–3032.

[22]. M. C. Payne, M. P. Teter, D. C. Allan, T. A. Arias, and J. D. Joannopoulos. Iterative minimization techniques for ab initio total-energy calculations: molecular dynamics and conjugate gradients. Rev. Mod. Phys., 64 :1045–1097, Oct 1992.

[23]. P. Hohenberg, W. Kohn. Inhomogeneous electron gas. Physical review, 136(3B): B864, 1964.

[24]. W. Kohn, L. J. Sham. Self-consistent equations including exchange and corre lation effects. Physical review, 140(4A): A1133, 1965

[25]. B. Erdmann, C. Keller, Actinide(lanthanide)-noble metal alloy phases, preparation and properties, Journal of Solid-State Chemistry, 7 (1973) 40-48, https://doi.org/10.1016/0022-4596(73)90119-9.

[26]. Hubbard, W. N., Rawlins, P. L., Connick, P. A., Stedwell Jr., R. E., & O'Hare, P. A. G. (1983). The standard enthalpy of formation of $LaNi_5$: The enthalpies of hydriding of $LaNi_5$−xAlx. The Journal of Chemical Thermodynamics, 15(8), 785–798. https://doi.org/10.1016/0021-9614(83)90145-3

[27]. Hubbard, W. N., Rawlins, P. L., Connick, P. A., Stedwell Jr., R. E., & O'Hare, P. A. G. (1983). The standard enthalpy of formation of $LaNi_5$ and the enthalpies of hydriding of $LaNi_5$−xAlx. The Journal of Chemical Thermodynamics, 15(8), 785–798. https://doi.org/10.1016/0021-9614(83)90145-3

[28]. Shimizu, Y., Otowaki, M., Shirai, K., & Ohyanagi, M. (2019). Consistency between the experimental formation entropy of MgH_2 and the spectroscopic entropy based on the third law of thermodynamics. Journal of Alloys and Compounds, 811, 152062. https://doi.org/10.1016/j.jallcom.2019.152062

الجمهورية الجزائرية الديمقراطية الشعبية
وزارة التعليم العالي والبحث العلمي

Université de Ghardaïa
Faculte des Sciences
et de la technologie

جامعة غرداية
كلية العلوم والتكنولوجيا
قسم :الآلية والكهروميكانيك

غرداية في :23/06/23

شعبة :العلوم والتكنولوجيا
تخصص: طاقات متجددة وبيئة

شهادة ترخيص بالتصحيح والايداع:

انا الاستاذ(ة) : بوحادة يوسف
بصفتي المشرف المسؤول عن تصحيح مذكرة تخرج (ليسانس/ماستر/دكتورا) المعنونة ب:
Solid-state hydrogen storage: Theoretical study of $ScPd_3H_4$ hydride
من انجاز الطالب (الطلبة):
بن غنية بشرى
ادريسي ايمان
التي نوقشت بتاريخ : 14/06/2026

اشهد ان الطالب/الطلبة قد قام /قاموا بالتعديلات والتصحيحات المطلوبة من طرف لجنة المناقشة وقد تم التحقق من ذلك من طرفنا
وقد استوفت جميع الشروط المطلوبة.

مصادقة رئيس القسم
رئيس قسم الآلية والكهروميكانيك
عزاوي محمد

امضاء المسؤول عن التصحيح
د. بوحـــادة يوسف
مسؤول فرقة
تقنية الهيدروجين